Journal of the Geological Society, *London*, Vol. **164**, 2007, pp. 621–636. Printed in Great Britain.

Superimposed folding and oblique structures in the palaeomargin-derived units of the Central Betics (SW Spain)

ANA CRESPO-BLANC

Departamento de Geodinámica, Instituto Andaluz de Ciencias de la Tierra, Universidad de Granada–CSIC, 18071 Granada, Spain (e-mail: acrespo@ugr.es)

Abstract: The Subbetic units consist of a deformed wedge of sedimentary rocks deriving from the South Iberian palaeomargin, in the westernmost segment of the Alpine–Mediterranean orogenic belt. In the central Betics, shortening produced folding, thrusting and nappe-stacking. The structural trend is NE–SW to ENE–WSW, and the internal structure of the thrust sheets, which shows no preferred vergence, is strongly controlled by the rheology of the décollement level, a viscous layer of Triassic evaporites, and of the overlying carbonate rock sequence. The relationships of piggyback basin Miocene sediments with the main structures show that the latter developed during the Aquitanian–Burdigalian transition. Superimposed folding is described for the first time in the study area. The origin of the interference cannot be determined at present, but may be related to initially oblique structures refolded during progressive deformation. A revision of previously published palaeomagnetic data in the light of the data presented in this paper, in conjunction with a model of the structural evolution of the Subbetic units of the western Betics, permits us to establish milestones of the tectonic evolution of the external zones in the northern branch of the Gibraltar Arc.

The westernmost segment of the Alpine–Mediterranean orogenic belt is generally known as a case study of collapse in the back-arc region of a subduction zone. Indeed, during the Miocene, the Betic–Rif orogen was affected by post-orogenic extension. The rifting that took place in the internal part of the Gibraltar Arc and led to the formation of the Alboran Basin occurred while an arcuate fold-and-thrust belt (now emerged) developed in its external part (e.g. Platt & Vissers 1989; Frizon de Lamotte *et al*. 1991; García-Dueñas *et al*. 1992). Over the past two decades, much attention has been paid to the extensional processes that affected the internal zones, but only a few papers have been published concerning the external zones. In particular, in the central and western Betics, which belong to the northern branch of the Gibraltar Arc, it is only recently that structural and kinematic data for the external zones have been published (Kirker & Platt 1998; Crespo-Blanc & Campos 2001; Luján *et al*. 2003, 2007; Platt *et al*. 2003; Frizon de Lamotte *et al*. 2004; Balanyá *et al*. 2007; Crespo-Blanc & Frizon de Lamotte 2006), excepting the paper of Blankenship (1992), which was immediately followed by three comments (Molina & Ruiz-Ortiz 1993; Reicherter 1993; Sanz de Galdeano *et al*. 1993).

In this paper, the structural evolution of the Subbetic units of the central Betics is described. These units were derived from the non-metamorphic sedimentary cover of the South Iberian palaeomargin, and the deformation style of this fold-and-thrust belt is strongly controlled by the rheological profile of the lithostratigraphic sequence of the deformed materials. A very complex fold-and-thrust geometry results from Early to Middle Miocene shortening. Oblique structures with respect to the main structural trend are frequent. Surprisingly, buckle fold interferences are observed. The data presented in this paper help us to fill a gap in knowledge of a tectonic domain whose structural evolution is generally sketched as a compressional front sweeping the external Betics area during Miocene times, and until now was a missing link in any model of the Gibraltar Arc tectonic evolution.

The Betic–Rif external zones within the Gibraltar Arc frame

The Betic and Rif chains, north and south of the Alboran Sea, respectively, together constitute an arc-shaped mountain belt, referred to as the Gibraltar Arc (Fig. 1 inset). This orogenic system developed during, and partly in response to, late Mesozoic to Cenozoic convergence between Africa and Iberia. Various tectonic domains can be differentiated within the Arc (Fig. 1). The Alboran Crustal Domain, considered as relicts of a former Alpine orogenic wedge and consisting mainly of three nappe complexes of variable metamorphic grade, occupies the inner part of the Arc (Balanyá & García-Dueñas 1988). The outer part is formed by the South Iberian and Maghrebian palaeomargins, which respectively belong to the southern part of the Iberian plate and northern part of the African plate. Both palaeomargins consist of non-metamorphic Mesozoic and Tertiary sedimentary cover, mainly detached during Miocene times from a Variscan basement, the Iberian and Moroccan Mesetas, respectively. A first event of stacking, Late Eocene in age, locally affected part of the Maghrebian palaeomargin. These detached sediments now form the Prebetic and Subbetic Domains in Spain, and the External Rif in Morocco. Foredeep basins, formed during middle and late Miocene times, fringe the orogenic system north and south of the Strait of Gibraltar. These are, respectively, the Guadalquivir and Pre-Rif Complexes, which finally evolved to foreland basins, the Guadalquivir and the Rharb Basins.

The Flysch Trough Units were derived from a basin with attenuated or oceanic crust filled by Jurassic to Miocene siliciclastic, deep-water sediments (Dercourt *et al*. 1986; Durand-Delga *et al*. 2000). This accretionary prism is now located in the western Betics and along the northern part of Africa from the Strait of Gibraltar to Tunisia (e.g. Dercourt *et al*. 1986), and separates the internal zone from the palaeomargin-derived units.

It is generally acknowledged that shortening in front of the Gibraltar Arc was due to the westward migration of the Alboran

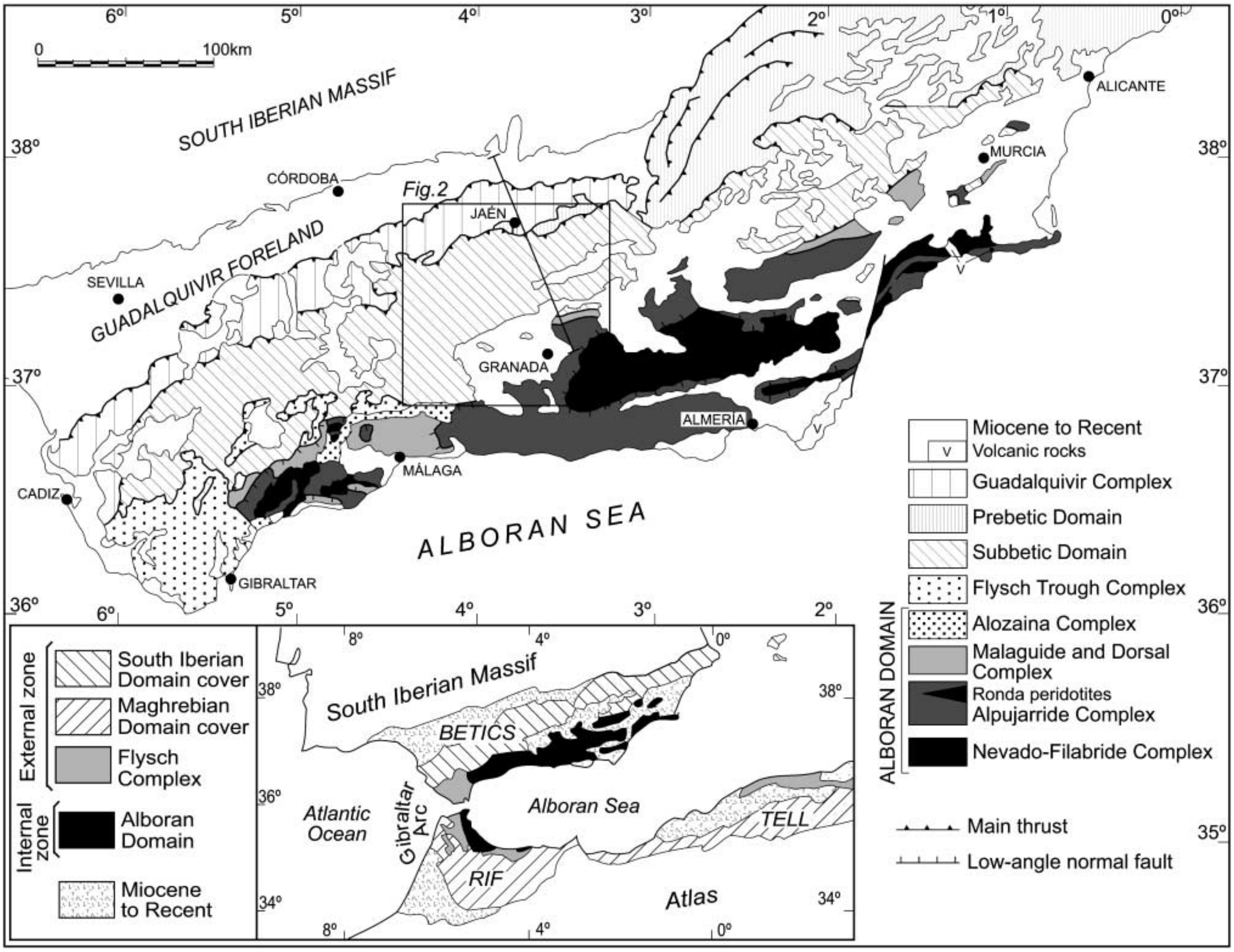

Fig. 1. Tectonic domains in the northern branch of the Gibraltar Arc. The inset shows the Alpine orogenic belts in the westernmost Mediterranean region.

Domain from Oligocene to Miocene times. Shortening obliterated the Flysch Trough and the outward migration of the compression resulted in the inclusion in the wedge of the sedimentary cover of the South Iberian and Maghrebian palaeomargins (Balanyá & García-Dueñas 1988). At the same time, extensional processes took place in the inner part of the Arc, leading to the Alboran Basin formation (Comas *et al*. 1999).

The South Iberian palaeomargin: a summary of the palaeogeography and lithostratigraphy

In the northern branch of the Gibraltar Arc, the detached cover of the South Iberian palaeomargin units formed allochthonous sheets, consisted of non-metamorphosed rocks of Triassic to Neogene age. Throughout the palaeomargin, the Triassic sediments show a 'germanic' facies, which ended with Late Triassic formation of gypsiferous claystones and fine-grained sandstones (Keuper facies). At the beginning of Jurassic times, a transgression took place and a broad shallow-marine environment developed. In the Early Jurassic, this carbonate platform broke down, leading to the differentiation of the Subbetic and Prebetic Zones from that time onwards (Fig. 1; García-Hernández *et al*. 1980). The Prebetic Zone is characterized by shallow-water facies, with continental deposits and/or erosional episodes, as opposed to the Subbetic Zone, where pelagic facies prevail. Moreover, in the Subbetic Zone of the central part of the Cordillera, three sedimentary realms have been distinguished: the External, Median and Internal Subbetic, according to palaeogeographical criteria and their position with respect to the emerged Variscan basement. The Median Subbetic is the realm that subsided most during Jurassic times, and has deposits of marls, pelagic limestones, radiolarites and calcareous turbidites, with mafic volcanic and subvolcanic rocks. In contrast, the External and Internal Subbetic are characterized by the absence of Jurassic radiolaritic facies. The Cretaceous is uniformly developed for the three realms (marls and marly limestones with pink pelagic limestones in the Late Cretaceous) and the Palaeogene is represented by very scarce outcrops of pelagic facies with interbedded turbidites and olistostromes.

Main structural features of the Subbetic Domain in the central Betics

Large-scale structural style

Shortening in the South Iberian palaeomargin units produced folding, thrusting and nappe-stacking, as illustrated by the large-scale cross-section of Figure 2. Various thrust sheets of palaeo-

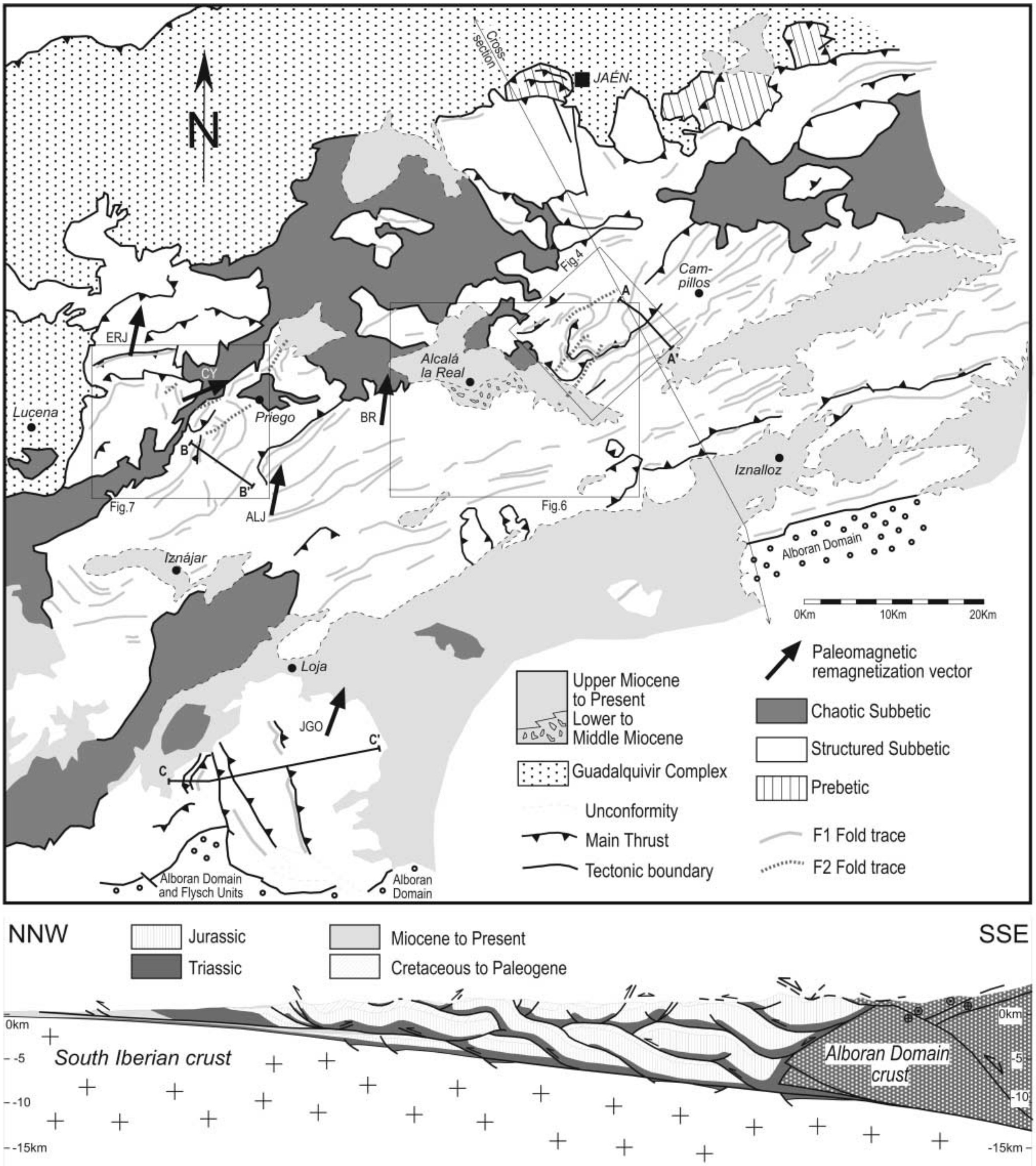

Fig. 2. Tectonic map of the Subbetic Domain in the central Betics (location shown in Fig. 1) and trend of the main structures associated with the main shortening. Palaeomagnetic remagnetization vector is according to Osete *et al*. (2004). Large-scale cross-section is according to Frizon de Lamotte *et al*. (2004). Location of the end points of the cross-section is shown in Figure 1.

margin-derived sedimentary rocks are superimposed, mainly in piggyback fashion. The widespread presence of Triassic evaporites, which can be recognized from geological maps (Junta de Andalucía 1985) and industrial well data (IGME 1987), imprints a particular structural style on the Subbetic fold-and-thrust belt. Indeed, considerable thicknesses of such materials have been drilled (up to 2600 m in the western Subbetic Domain; IGME 1987). These viscous rocks represent the main detachment level, and are responsible for the lack of cylindrical structures in the Subbetic Domain, similar to other cases of fold-and-thrust belts detached over evaporites (e.g. the Jura in front of the Alps, Sommaruga 1999; the Salt Range in Pakistan, Butler *et al*. 1987;

Cotton & Koyi 2000; the Zagros Mountains in Iran, Bahroudi & Koyi 2003).

In wide areas of the Betics, the internal structure of the Subbetic units can be chaotic, as a result of the extreme plasticity of the evaporitic rocks: kilometre- to decimetre-scale blocks of Jurassic to Cretaceous carbonate rocks are randomly embedded in a claystone and gypsiferous matrix (Triassic Keuper facies). Accordingly, in the study area, the Subbetic Domain has been differentiated into 'structured' and 'chaotic' Subbetic (Fig. 2; see also Vera 2004). The trend of the structures within the coherent Subbetic fold-and-thrust belt of the central Betics is illustrated in the tectonic map of Figure 2. It is mainly NE–SW to ENE–WSW directed, similar to the trend of the Guadalquivir foreland basin, although in some areas the trend lines of this map also indicate oblique structures and superimposed folding (e.g. south of Loja, ENE of Alcalá La Real and west of Priego, Fig. 2). These peculiar structures are characteristic of the Subbetic Domain that crops out in the central Betics and will be described in detail below.

The cross-section of Figure 2, the so-called Granada transect, illustrates the structural style of the Subbetic Domain in the central Betics. It is based on the study by Frizon de Lamotte *et al*. (2004), who gave a complete discussion of its geometry. The position of the cross-section line has been selected to avoid the chaotic Subbetic, and to cross nearly cylindrical structures that can be followed over tens of kilometres. It must be stressed that, although carefully drawn, it is not intended as a strictly balanced cross-section.

The north-northwesternmost segment of the section of Figure 2 is situated a few kilometres from the boundary of the Variscan basement with the Guadalquivir Basin, the early Tortonian to Pliocene foreland basin. Towards the south, the so-called Guadalquivir complex crops out. It consists of a Miocene foredeep basin composed by Subbetic rock olistoliths within a marly matrix dated as Burdigalian to Serravallian; that is, contemporaneous with the main episode of the Subbetic fold-and-thrust belt formation (Martínez del Olmo *et al*. 1984; Sierro *et al*. 1996; Vera 2000). These olistrostromic deposits are present mainly in the eastern part of the complex, whereas in the western part a chaotic mixture of Triassic evaporites with scattered younger rocks appears. The chaotic mixture of Triassic evaporites is highly deformed and has been interpreted either as a Miocene accretionary wedge intruded by squeezed diapirs of Triassic evaporites (Berástegui *et al*. 1998; Fernàndez *et al*. 1998), or as a tectonic wedge with overthrusting evaporites emplaced during the Late Cretaceous–Palaeogene (Flinch *et al*. 1996).

The depth of the South Iberian Variscan basement has been drawn according to commercial wells and seismic data (IGME 1987). Towards the SW, below the Subbetic Domain, the boundary between the Variscan basement and the cover has been extrapolated. The shallower levels of the Subbetic units are constructed from the available geological maps (1:50 000 MAGNA Spanish series). Accordingly, the cross-section is fairly well constrained down to a depth of about 2 or 3 km. At greater depth, the structure is more speculative, although it follows the common rules of fold-and-thrust belt geometry.

Within the Subbetic units, the youngest pre-tectonic rocks with respect to the main folding and thrusting event are Aquitanian in age. Syntectonic Miocene sediments deposited in piggyback basins, such as those that crop out around Alcalá la Real (Fig. 2), show that the main shortening took place close to the Aquitanian–Burdigalian boundary (e.g. Bourgois 1978; Soria 1994), although pulses of compressional deformation continued to Late Tortonian times (see below).

Finally, in the southernmost part of the cross-section, the geometry of the boundary between the Alboran Domain and the Subbetic Zone deformed wedge has been drawn according to field and gravity data (see complete discussion by Frizon de Lamotte *et al*. 2004).

Detailed cross-sections: geometry constrained by the rheological profile of the deformed Subbetic sequences

The geometry of the cross-section presented above shows the main structure of the external zones in the central Betics on a large scale. To draw such a long cross-section and reduce it to a publishable size called for some simplification of the geometry of its uppermost level. A detailed view is needed to characterize the representative mesoscale structure of the Subbetic units in the study area.

Detailed cross-sections of the uppermost thrust sheet of the Subbetic units are presented in Figure 3. These cross-sections were drawn across folds and thrusts that can be followed for at least 15 km (Fig. 2). Only the upper part of the sections was drawn, as it is well constrained by the surface geology. Cross-sections A–A′ and B–B′ are NW–SE oriented (i.e. subperpendicular to the main structural trend); whereas cross-section C–C′ is WSW–ENE oriented, as it crosses the area situated south of Loja, where the trend is anomalously directed (Fig. 2). The deformation style of the folds and thrusts is strongly controlled by the rheology of the lithostratigraphic sequences, which appear in parallel with the cross-sections.

The synthetic lithostratigraphic columns of the Alcalá La Real (hereafter Alcalá) and Priego de Córdoba (hereafter Priego) areas are common for the Triassic and early Jurassic age interval (Fig. 3). They are characterized by a viscous layer of Triassic evaporites, overlain by highly competent dolomitic rocks of Liassic age. In contrast, the lithostratigraphy of the Middle and Upper Jurassic units differs from one place to another, depending on whether the folded units belong to the Median or to the External Subbetic. Moreover, within these domains, lateral variations in sedimentary facies are common. East of Alcalá the rocks belong to the Median Subetic and the Liassic rocks are overlain by a less competent layer characterized by an alternation of limestones and marly rocks (Middle Jurassic), in which intrusions of basaltic volcanic rocks are sometimes abundant. On top of this sequence a relatively thin layer of radiolaritic rocks, of Late Jurassic age, appears. Nodular limestones of late Jurassic age can also be found. In the area west of Priego, the transition between the Median and External Subbetic Domain can be observed: the lithostratigraphy is more variable, as shown in Figure 3. Finally, on top of the sequence, less competent marls and marly limestones of Cretaceous to Palaeogene age appear, common to both the Median and External Subbetic.

Consequently, the rheological model for the Alcalá and Priego areas can be broadly considered as a three-layer model composed of, from bottom to top, a viscous layer of evaporitic rocks (more than 100 m thick), a highly competent layer of dolomitic rocks (around 250 m thick), and a less competent layer of alternating of marls, marly limestones or limestones (800–1000 m thick). Shortening of such a rheological sequence gave rise to a particular style of deformation, which characterizes many areas of the structured Subbetic Domain. In cross-sections A–A′ and B–B′ of Figure 3, the folds and thrusts show no preferred vergence. Faulting and folding, which regionally define box-folds with associated pop-up and pop-down structures, are observed. Thrust ramps frequently cut across the limbs of the box-folds,

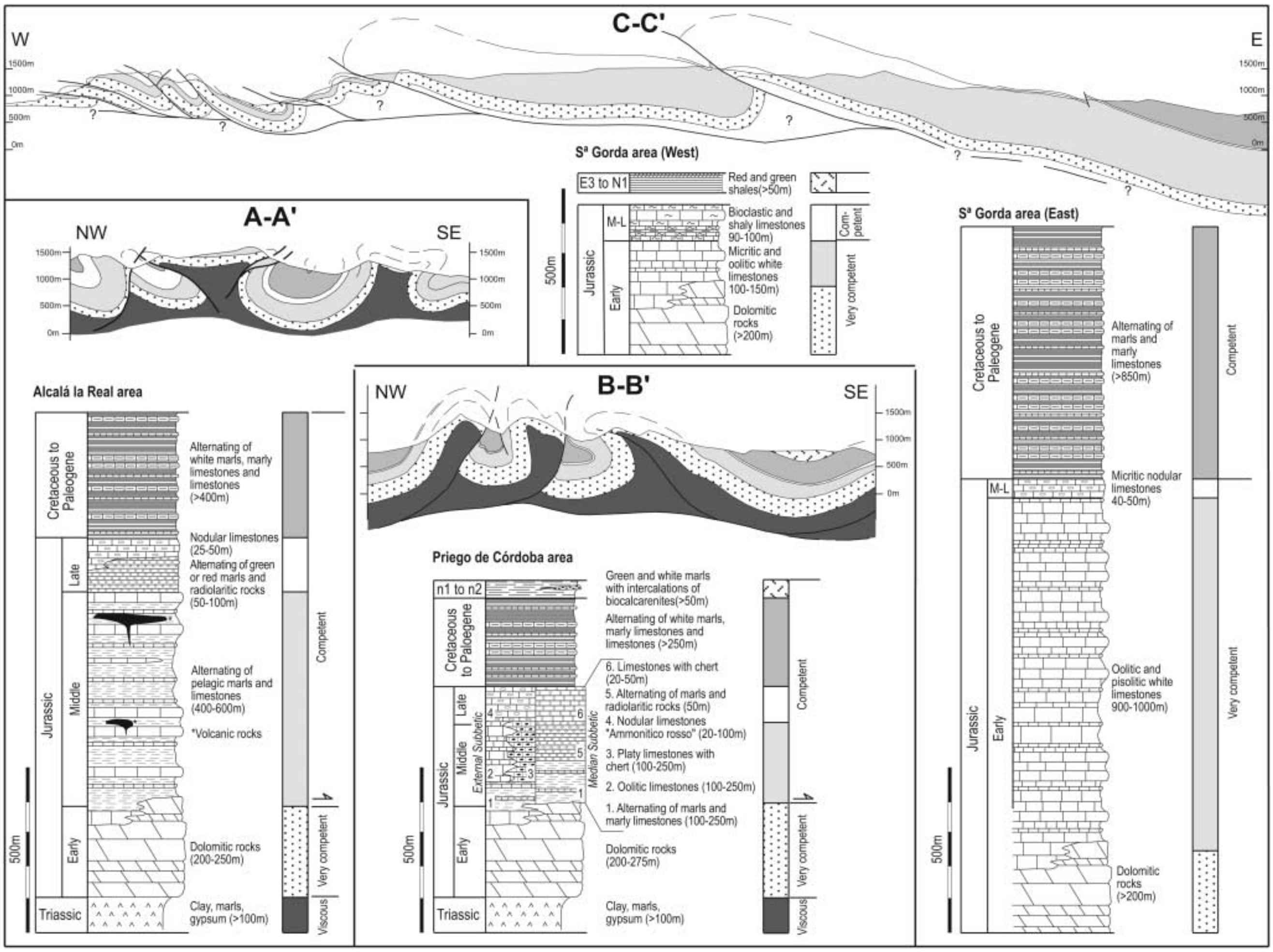

Fig. 3. Detailed cross-sections characteristic of the structural style of the Subbetic units in the central Betics, and synthetic lithostratigraphic succession of the Subbetic units in the areas where the cross-sections have been drawn. A–A′, Alcalá la Real area; B–B′, Priego de Córdoba area; C–C′, Sierra Gorda de Loja area. The column labelled 'Sª Gorda (East)' corresponds to the lithostratigraphy of the two thrust sheets situated in the eastern part of the cross-section. To clarify the differences of lithostratigraphic sequence and structural style of the cross-sections, the same scale has been used for the columns and the cross-sections, respectively. E3, Oligocene; N1, Miocene, n1– n2, Aquitanian–Burdigalian. Location of the cross-sections is shown in Figures 4, 6 and 2, respectively.

which eventually underwent either foreland- or hinterland-directed thrust breakthrough and translation.

The geometry and structural style of the previous cross-sections strongly contrasts, in terms of vergence and thickness of the involved material, with those of Sierra Gorda, south of Loja. Cross-section C–C′ shows a west- to WSW-vergent thrust system whose basal detachment does not reach the surface (Fig. 3). In this case, Triassic rocks do not crop out at the bottom of the thrust sheet. Its western part is characterized by two huge slices, around 10 km long, whereas in the eastern part much shorter thrust slices appear (less than 1 km). This striking difference is related to the thickness of the lithostratigraphic columns and their corresponding rheological profiles (Fig. 3). In its western part, the lithostratigraphic sequence is very thin and is made up of a highly competent unit of massive carbonate rocks overlain by competent limestones. Atop, incompetent shales can be found. By contrast, in its eastern part, a highly competent unit of dolomites and limestones appears, with a thickness reaching at least 1200 m. It is overlain by a 700 m thick, less competent layer of alternating marls and marly limestones. It must be emphasized that the substrate below the thrust system is not known, in either the eastern part or the western part of the profile.

Superimposed folding and oblique structures

The presence of a viscous substrate below the Subbetic deformed wedge enhances the fact that the structures are often not cylindrical. Independently of this lack of lateral continuity, the mapping of the structural trend of the 'structured' Subbetic units of the central Betics reveals the presence of anomalous areas where the trend lines differ from the normal NE–SW to ENE–WSW direction (Fig. 2). As the topography of the region covered by Figure 2 is relatively smooth, these variations in orientation are not due to an intersection effect between the thrust planes or fold axial surfaces and a rugged topography. Therefore, the variation of trend-line orientation reveals the presence of either superimposed folding or oblique structures.

Buckle fold interferences in the central Betics are described for the first time in this paper. Two areas are of particular interest for the discussion of such a remarkable superimposition of structures: (1) the area situated east of Alcalá, because the

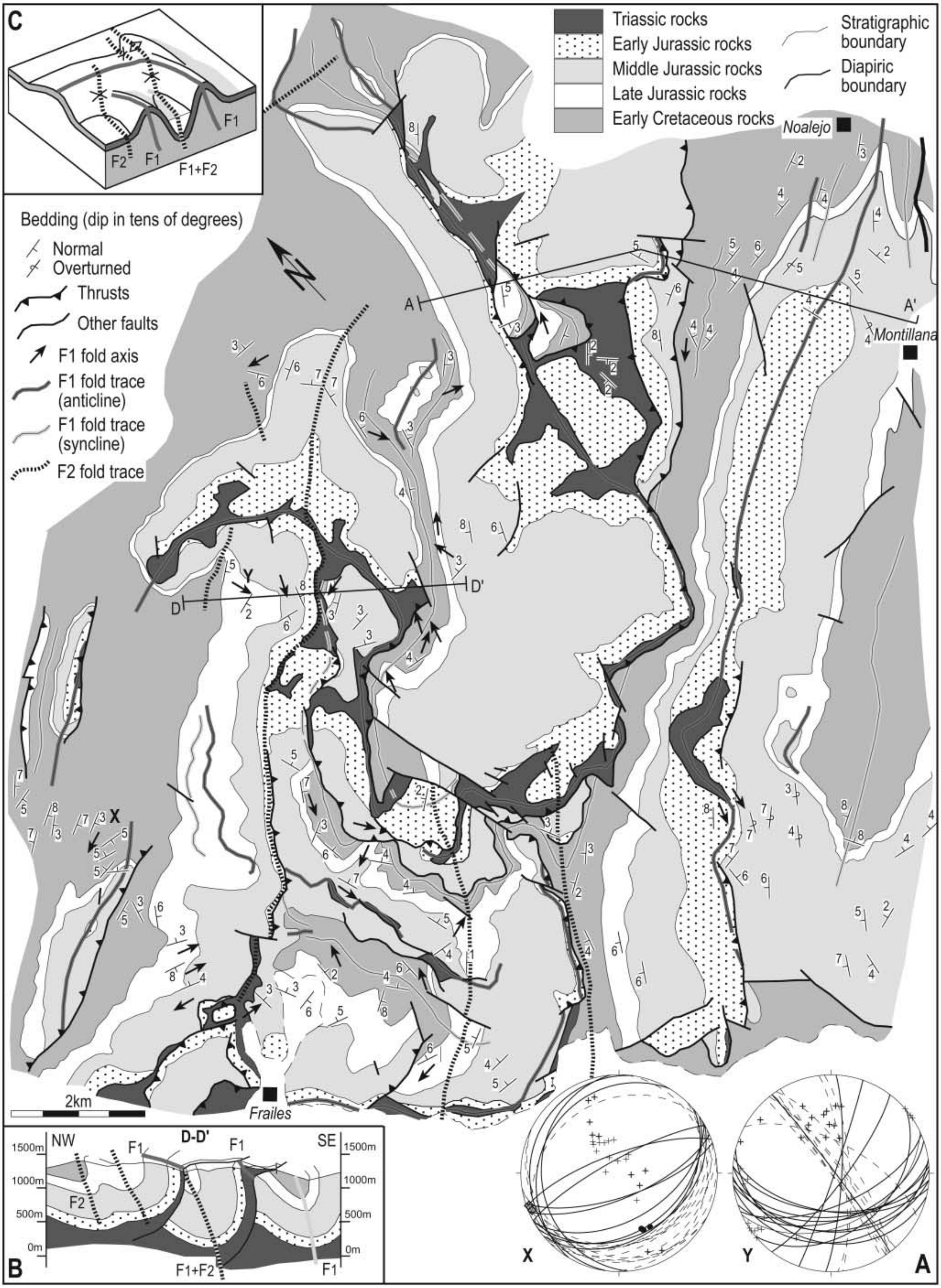
C
F1
F2
F1
F1+F2
Triassic rocks
Early Jurassic rocks
Middle Jurassic rocks
Late Jurassic rocks
Early Cretaceous rocks
Stratigraphic boundary
Diapiric boundary
Bedding (dip in tens of degrees)
Normal
Overturned
Thrusts
Other faults
F1 fold axis
F1 fold trace (anticline)
F1 fold trace (syncline)
F2 fold trace
N
Noalejo
Montillana
A
A'
D
D'
X
Y
Frailes
2km
NW
D-D'
SE
1500m
1000m
500m
0m
F1
F2
F1+F2
B
X
Y
A

folding chronology can be constrained from the relationships between folds and piggyback sediments; (2) the area west of Priego, where the fold superimposition allows us to constrain the relative age of the vertical-axis rotations determined by palaeomagnetic methods (Fig. 2). Concerning the oblique structures, the west- to WSW-vergent thrust system of Sierra Gorda, in the southwesternmost part of the map of Figure 2, represents a key structure to elucidate the role of the vertical-axis rotations indicated by palaeomagnetic data published in a previous paper (see the Discussion and references therein). It can be followed laterally for 20 km.

It must be stressed that superimposed folding in external zones implies processes of buckling, in which the variations in rheological properties along the lithological sequence control the fold geometry. Consequently, the classic fold interference model proposed by Ramsay (1967), involving passive or shear folding, cannot be directly applied to explain buckle superimposition. Indeed, when layers are mechanically active during refolding, the geometry of superimposed buckling depends to a large extent on the initial shape of early folds, as early hinges represent a structural anisotropy that strengthens the materials (Ghosh & Ramberg 1968; Skjernaa 1975; Watkinson 1981; Ghosh *et al*. 1992; Grujic 1993; Grujic *et al*. 2002; Sengupta *et al*. 2005). In this paper, the classification of superimposed buckle folds developed by Simón (2004) will be used. It follows the criteria proposed by Ghosh & Ramberg (1968), Skjernaa (1975), Thiessen & Means (1980) and Ghosh *et al*. (1992), but uses a slightly modified nomenclature. In the study area, dome-and-basin and crescent-type interferences have been observed (Type 1a and 2a of Simón 2004, respectively; see sketches in Figs 4 and 6).

Alcalá la Real superimposed folding: a detailed map

West of the Alcalá area, the complex geometry of box-folds with frequent inverted limbs and forelandward or hinterlandward thrust, which resulted from the first folding phase (F_1; cross-section A–A′ of Fig. 3), is affected by a second folding phase (F_2). The resulting geometry is shown in the detailed structural map of Figure 4a, which illustrates spectacular, mushroom-type fold interference. The complexity of the pre-existing structures involved in the fold interference is illustrated in the cross-section D–D′ (Fig. 4b), although along this profile the F_1 structures have been tightened by the F_2 folding phase. Indeed, the interference is indicated mainly by (1) F_1 synclines with very highly dipping to subvertical axial planes, as shown by bedding measurements, and (2) the nearly horizontal limbs of the upper part of the box-folds, generally detached from one of the fold limbs. In cross-section D–D′, the central syncline has been popped down and its axial plane capped by the subhorizontal part of a box-fold anticline.

The axial traces of both generations of folds are drawn in both the map and cross-section D–D′ (Fig. 4a and b, respectively). F_1 and F_2 folds have similar, kilometre-scale wavelengths, and small-scale fold interference has not been observed. The main F_1 folds are much more frequent than the F_2 folds, and are characterized by lack of lateral continuity. Various F_1 synclines or anticlines nucleate in the area of superimposed folding and relay each other. A 3D sketch of the mushroom-type interference in the northwestern part of the structural map has beeen drawn (Fig. 5c), although the box-folds present in the study area have been simplified and represented as simple anticline and syncline. The F_1 axial traces, NE–SW-directed in the northeastern part of the map, can be followed within the fold interference, where the traces swing towards a NW–SE direction. The axial traces of the pop-down synclines have been drawn discontinuously below the thrust that hides them (compare Fig. 4a and 4b). The distribution of the axial traces of both the F_1 and F_2 folds involves the bending of the subvertical axial surfaces of the early folds, and refolding of originally subhorizontal F_1 hinges within the horizontal plane. Consequently, a 2a-type interference is drawn (Simón 2004).

When a crenulation cleavage is present (as, for example, in hinge zones marked by marly rocks) it is related to the folds considered to belong to the first phase, as it shows coherent relationships with F_1 folds. For instance, structural elements plotted on stereoplot X (Fig. 4) have been measured in an area where only hectometre-scale F_1 folds are present. The F_1-axis deduced from the intersection of the plotted bedding planes is subhorizontal and ENE–WSW directed. It also corresponds to the intersection of the crenulation cleavage, which in turn approximately corresponds to the axial plane of the F_1 fold. In contrast, stereoplot Y was measured in the area of superimposed folding. It shows similar geometric relationships between bedding and crenulation cleavage, but in this case the F_1 folds have been rotated and are now NNW–SSE directed.

Relationship of the Alcalá piggyback deposits with the superimposed folding

The timing of the superimposed structures described above can be constrained by analysing their relationships with syntectonic Miocene deposits belonging to piggyback basin installed above the deforming Subbetic Domain. Such relationships can be observed close to Alcalá, situated west of and adjacent to the fold interferences mapped in Figure 4. A detailed structural map of this basin, together with the lithostratigraphic column of its syn- to post-tectonic deposits, is given in Figure 5.

The age of the Miocene rocks that appear in the lithostratigraphic column of Figure 5 is well constrained, as the rocks have been dated using nannoplanktonic and foraminiferal faunas (Díaz de Neira *et al*. 1991*a*, *b*; López Olmedo *et al*. 1991). No synsedimentary normal fault has ever been observed in these materials, and the deposits affected by some compressional deformation range from Late Aquitanian to Pliocene in age. Only the Pleistocene to Present deposits are clearly post-tectonic. The late Burdigalian conglomerates are considered to be related to

Fig. 4. (**a**) Structural map of the superimposed folds observed in the central Subbetic Domain, east of Alcalá la Real (location shown in Fig. 2). The geological map is based on Díaz de Neira *et al*. (1991*a*) and López Olmedo *et al*. (1991). It should be noted how the southernmost axial traces of F_2 syncline can be followed within the piggyback basin rocks (see Fig. 6). The stereoplots show a cyclographic projection of bedding (continuous lines) and crenulation cleavage (dotted lines), measured in mesoscale F_1 folds (location indicated on the map by bold letters); the corresponding poles are plotted as bold and fine crosses, respectively. Stereoplot X: ●, calcite fibres within bedding, indicating a flexural slip mechanism; ■, metric-scale F_1 fold axes. Cross-section A–A′ is shown in Figure 3. (**b**) Cross-section D–D′ illustrating the F_1 + F_2 fold interference geometry in an area where the two axial traces are parallel (drawn and labelled on the cross-section). The very highly dipping axial planes of the synclines and the normal, nearly horizontal limbs in the upper part of the box-folds should be noted. (**c**) A 3D sketch of the mushroom-type interference in the northwestern part of the map (type 2a of Simón 2004).

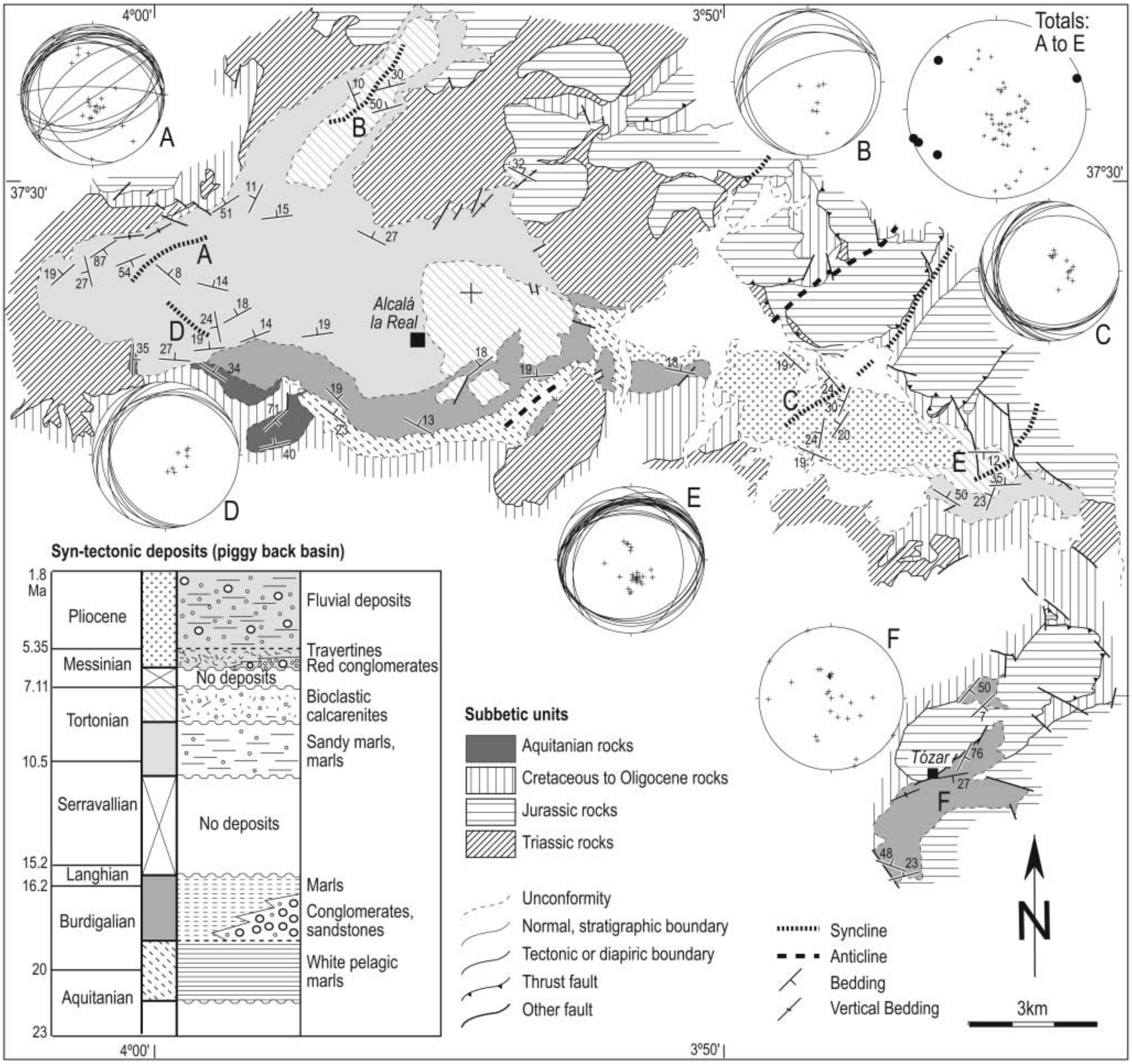

Fig. 5. Structural map of the Alcalá la Real piggyback basin and corresponding simplified lithostratigraphic column, which includes the legend for the map. The syntectonic deposits are late Aquitanian to Pliocene in age, whereas the Pleistocene to Present sediments (unshaded) can be considered as post-tectonic. The geological map and stratigraphic data are based on Díaz de Neira *et al*. (1991*a*), García-Cortés (1991) and López Olmedo *et al*. (1991). It should be noted that the northeasternmost syncline axial traces can be followed within the Subbetic rocks (see Fig. 4). The stereoplots show cyclographic projection and pole of bedding. Stereoplot totals: ●, mean fold axes based on stereoplots A–E.

the uplift and erosion of the new topographic reliefs associated with the active mountain front (Rodríguez-Fernández 1982; Díaz de Neira *et al*. 1991*a*, *b*; López Olmedo *et al*. 1991; Soria 1994, 1998; Vera 2000). Two gaps, representing the Late Langhien–Serravallian and Early Messinian, are present in the area, and from the Late Miocene onwards a clear continentalization of the basin took place (Rodríguez-Fernández 1982; Díaz de Neira *et al*. 1991*a*, *b*; López Olmedo *et al*. 1991; Soria 1994, 1998; Vera 2000). In the field, small angular unconformities separating one formation from another can be observed.

The oldest deposits sealing the main deformation episodes are of Late Aquitanian to Early Burdigalian age, as they lie unconformably over most of the structures formed by the Subbetic rocks (Fig. 5). In particular, they fringe the southern part of the Alcalá la Real basin and seal a closed NE–SW-trending syncline, marked by rocks dated to the Aquitanian belonging to the Subbetic units (Díaz de Neira *et al*. 1991*a*). Consequently, in this area the main deformation episode took place close to the Aquitanian–Burdigalian boundary. However, shortening continued during Miocene times. Indeed, systematic measurements of bedding within sedimentary rock of the Alcalá piggyback basin show that hectometre- to kilometre-scale smooth folding took place.

Stereoplots A–F of Figure 5 are for measurements made in

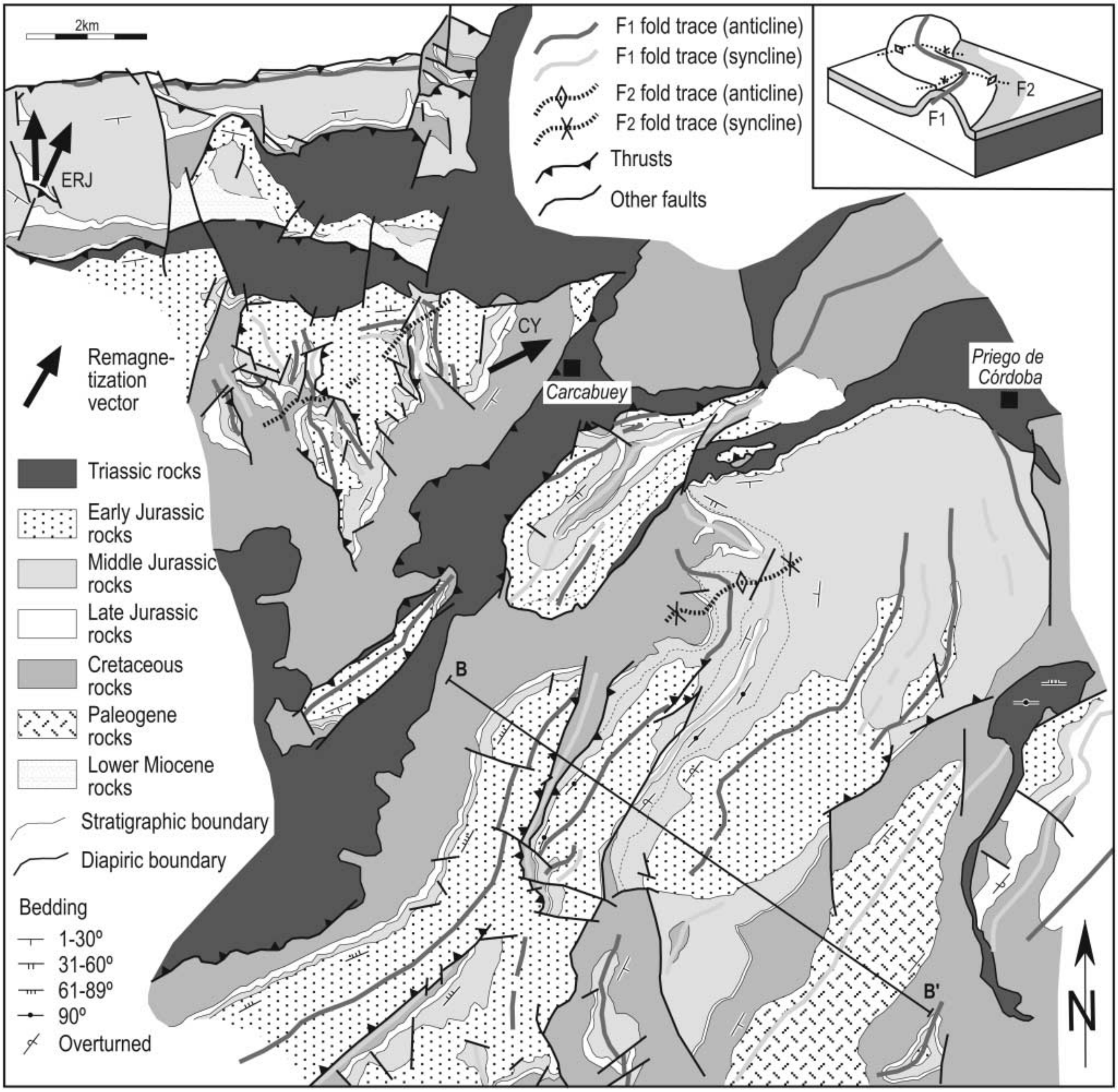

Fig. 6. Structural map of the superimposed folds observed in the central Subbetic Domain, in the Priego de Córdoba area. The geological mapping is based on Hernaiz Huerta *et al*. (1991). Cross-section B–B′ is shown in Figure 3. Remagnetization vector is according to Osete *et al*. (2004). The inset is a 3D sketch of the fold interference of the central part of the map (type 2a of Simón 2004).

Upper Burdigalian to Pliocene rocks. Coherent domains have been selected, to show hectometre- to kilometre-scale folds. Stereoplots A (bedding measured in Lower Tortonian rocks), B, E (bedding measured in upper Tortonian rocks), and C (bedding measured in Upper Messinian to Pliocene rocks) show NE–SW-trending folds, whose axes have been drawn in Figure 5. These folds are gentle to very open, with an interlimb angle that varies between 120 and 150°. Most of the measurements correspond to slightly dipping stratification planes, but vertical bedding can be observed locally; for example, along the northwestern border of Alcalá la Real basin. No appreciable difference could be seen in the interlimb angle as a function of the age of a given formation, which would have indicated a progressive fold tightening. It is noteworthy that in the easternmost part of the Alcalá map, at least two NE–SW-trending syncline traces can be followed from the Early to Late Miocene piggyback basin to the folded Subbetic rocks (Fig. 5). It is deduced that smooth folding of the piggyback sediments was accompanied by tightening of the NE–SW-directed folds present in the Subbetic units.

Stereoplot D shows a gentle, decametre-scale NW–SE-directed syncline in Lower Tortonian rocks. It is the only fold with this trend measured in the piggyback deposits. The bedding orientation of the southern border of the basin, a few kilometres south and SW of Alcalá (in Middle Miocene rocks), or that of its eastern extremity (in Upper Miocene deposits), is coherent with such a fold-axis direction.

The presence of nearly perpendicular NE–SW- and NW–SE-trending folds, together with the bedding orientation shown by the structural mapping of the piggyback deposits, is in agreement with the presence of dome and basin interference. The folds involved in the interference are gentle and a much higher frequency of NE–SW-trending folds is observed. The bedding pole dispersion around a great circle, which is ENE–WSW-oriented (stereoplot totals A–E of Figure 5), is probably due to this fold interference. In the same plot, the mean fold axes determined in plots A–E are shown. Unfortunately, the poor outcrops of the Alcalá area do not allow for the establishment of the chronology of folding phases.

Around Tózar, in the southeastern corner of Figure 6, the bedding in Upper Burdigalian to Lower Langhian rocks also indicates basin interference. The structure consists of a refolded NE–SW-oriented syncline, whose axis is horizontal in the central part of the syncline but moderately plunging in the southwestern part. In this area, NNE–SSW-directed metre-scale folds, with an interlimb angle of about 90°, are occasionally seen. The plot of all the bedding pole measurements made in the Tózar area shows a similar dispersion to the total A–E stereoplot for Alcalá (Fig. 5).

Superimposed folding west of Priego

In the area near Priego where buckle superimposed folding is present, the lithostratigraphic transition from the Median to the External Subbetic can be observed. However, as the rheology of the column of deformed rocks is similar (Fig. 3), this has no effect on the structural style. Hence, the two domains are not differentiated in the structural map of Figure 6. In this area, the F_1 main folds are NE–SW trending in the southern part of the map, and east–west trending in the northernmost part. Two axial traces of F_2 folds, which are NE–SW directed, produced the bending of the subvertical axial planes of F_1 folds, in particular of the syncline–anticline pair appearing in the central part of the cross-section B–B′ of Figure 3. This bending is not as so sharp as at Alcalá, as the shortening caused by the second phase near Priego is probably less pronounced. Indeed, the F_2 fold wavelength differs in the two areas: whereas it is some 4 km around Alcalá, it is almost 10 km near Priego. Moreover, where the F_2 axial traces can be drawn, the F_1-affected structures are folds in which no hinterland- or foreland-directed thrusts appear along the flanks. Each F_2 anticline or syncline on a limb of the F_1 fold continues, respectively, as a syncline or anticline on the other limb of the F_1 fold (see sketch in Fig. 6 inset). Accordingly, these can be classified as 2a fold interference (Simón 2004).

In the case of Priego, the only constraint for the timing of deformation is related to the Lower Miocene (Aquitanian to Burdigalian) marls involved in the east–west-directed thrust, whichc was associated with the main shortening event in the northernmost part of the map. In turn, these sediments are clearly discordant over the underlying Mesozoic to Palaeogene rocks.

Oblique structures of Sierra Gorda south of Loja

The north–south to NNW–SSE structural trend of Sierra Gorda is an anomaly within the NE–SW to ENE–WSW trend developed in the Subbetic units of the central Betics (Fig. 2). The structural style here is strikingly different from that of other areas of the central Betics, which show a bi-vergent box-fold type structure. Sierra Gorda is characterized by a west- to WSW-vergent imbricate thrust system that can be followed laterally for 20 km, and that is not affected by superimposed folding (Figs 2 and 3). The only age constraint for the thrust imbrication is represented by the Tortonian subhorizontal sedimentary rocks that crop out east and north of Sierra Gorda (Lupiani *et al*. 1988).

Towards the north, the Sierra Gorda imbricated slices are bounded by Triassic evaporites belonging to the so-called chaotic Subbetic, which are in turn overlain by subhorizontal Pliocene sediments. Towards the south, it is bounded by Alboran Domain and Flysch Trough units, along a nearly rectilinear east–west shear band that can be followed to the west, as far as the NE–SW-trending structures of the Subbetic units of the western Betics (Fig. 7). The Miocene sediments found along this boundary (the Alozaina complex of Fig. 7), led Balanyá *et al*. (2007) to interpret this shear band as a dextral strike-slip corridor, in which faults and folds developed between the Late Burdigalian and Early Tortonian (Barba *et al*. 1979; Martín-Algarra 1987; Cano Medina & Ruiz Reig 1990*a*).

Discussion

Constraints on timing of deformation

The relationships of the Miocene sediments of the Alcalá piggyback basin with the structured Subbetic units (Fig. 5) show that, in the Alcalá area, the main deformation episode generating the NE–SW- to ENE–WSW-directed main folds took place close to the Aquitanian–Burdigalian transition. In the central Betics, previous studies dated the development of the Subbetic Domain fold-and-thrust wedge to Burdigalian times, although tightening of the pre-existing structures could have occurred during the Middle and Late Miocene (Comas 1978; Estévez *et al*. 1982; Comas *et al*. 1986; Martín Algarra *et al*. 1988; Alvaro *et al*. 1991; Díaz de Neira *et al*. 1991*a–c*; Guerrera *et al*. 1993; Soria 1994, 1998; Vera 2000). In fact, the age of this main deformation episode can be refined, in view of the age of the foredeep olistostromic deposits, which were derived from the erosion of the relief associated with the active mountain front. A migration of the compressional deformation front can be deduced, as these deposits are early Burdigalian in age in the southernmost part of the central Subbetic Domain and Serravallian in the northernmost outcrops (Comas 1978; Vera 2000). This implies a migration of the main deformation front of about 50 km during a 5–6 Ma interval.

The superimposed folding in the Subbetic Domain that crops out in the central Betics is described as such for the first time in this paper, raising the question of the age of the second fold phase. It has been shown that the Alcalá piggyback basin sedimentary rocks show smooth basin and dome fold interference, in which the most frequent folds are NE–SW directed. Part of these smooth folds, post-Early Burdigalian, nucleate over some F_1 main folds in Subbetic units (Fig. 5), yet they are so open that they are probably insufficient to produce the severe superimposed folding described east of the Alcalá basin. It is therefore suggested that the interference began during the F_1 main folding episode, in Early Miocene time. In fact, 20 km west of Alcalá, an isolated fold interference structure surrounded by Triassic evaporites is sealed by Upper Burdigalian to Langhian rocks, which in turn are slightly folded (NE–SW- to ENE–WSW-directed, very open folds) (Díaz de Neira *et al*. 1991*b*).

Did the fold interference occur over oblique structures?

Oblique structures and, above all, superimposed folding in the Subbetic Domain that crops out in the central Betics are peculiar.

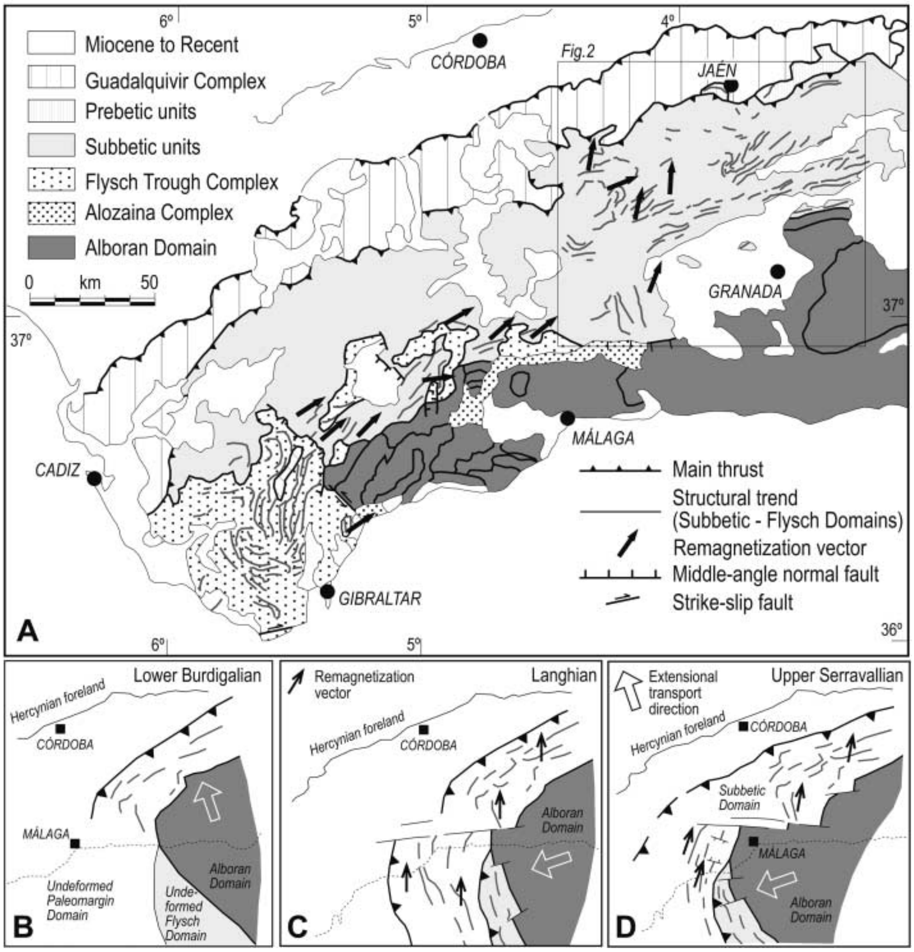

Fig. 7. (**a**) Map of the structural trend in the Subbetic and Flysch Trough Domains; according to this study for the central Betics, and Crespo-Blanc & Campos (2001) and Luján *et al*. (2006) for the western Betics. Medium-angle normal faults and strike-slip faults are structures that produce arc-parallel stretching in the western Betics, according to Balanyá *et al*. (2007). Remagnetization vector is according to Villalaín *et al*. (1994, 1996), Kirker & McClelland (1996) and Osete *et al*. (2004). Sketches in the upper part of the map show three stages of the structural evolution of the Gibraltar Arc northern branch: (**b**) Early Burdigalian; (**c**) Langhian; (d) Late Serravallian. The approximate position of the coastline (dotted line) and the towns of Cordoba and Malaga are shown for reference.

The presence of evaporitic rocks as the substrate of the Subbetic fold-and-thrust belt, which favours the absence of cylindrical structures, is probably not unfavourable to the development of oblique structures but in itself is not sufficient to produce fold interferences. Indeed, superimposed buckle folding arises only when shortening affects pre-existing folds in such a way that the trend of the early structures is nearly perpendicular to the later stress direction (Ghosh & Ramberg, 1968). It must be stressed that if this angle is not correct, the earlier buckle folds rotate (hinge migration of Odonne & Vialon 1987).

At the moment, only working hypotheses on the origin of both oblique structures and superimposed folding can be formulated. The simplest is that these structures are due to two different, successive compressional directions, which must have been almost perpendicular. This proposal, extrapolated to the geological situation of the Subbetic units of the central Betics, would imply an initial NE–SW to ENE–WSW compressional direction and a subsequent NW–SE to NNW–SSE direction of compression (subperpendicular to the F_2 fold axial planes, Fig. 2). This is difficult to frame within the tectonic evolution of the external zones, as no NE–SW to ENE–WSW compression has been recognized in the central Betics. The only similar direction is the east–west compression that gave rise to the westernmost corner of the Prebetic wedge, but the imbrication is dated as Late Miocene (area of Cazorla, about 100 km east of Jaén, Fig. 1) (Guezou *et al*. 1991; García-Hernández *et al*. 2004). This is not in agreement with the data presented in this paper, as the age constraints suggest that both folding episodes took place during a very short time interval, the first episode close to the Aquitanian–Burdigalian boundary and the second before the Late Burdigalian–Langhian. Moreover, oblique structures and superimposed buckle folding as a result of two different, successive compressional directions would have probably developed a more frequent, regularly distributed superimposition of structures, and not the localized interferences observed in the central Betics.

A second working hypothesis (my preferred interpretation) is that oblique folds and thrusts could have locally developed in the earliest stages of the progressive deformation. Then, the pre-existing oblique structures were subsequently folded, as a result of local variation of the stress field orientation, until there was almost parallelism between the pre-existing fold trend and the maximum compression axis. If this working hypothesis is correct, we first need to generate oblique structures in the deformed wedge. Analogue models consisting of a homogeneous layer of silicone overlain by sand and pushed by a straight, rigid backstop do not generate oblique structure when compression occurs along a single direction (e.g. Costa & Vendeville 2002). Accordingly, we would require the presence of: (1) heterogeneities in the substrate (e.g. Bahroudi & Koyi 2003; Luján *et al*. 2003; Affolter & Gratier 2004; Likorish *et al*. 2002); (2) heterogeneities in the folded sequence (e.g. Soto *et al*. 2002, 2003); (3) heterogeneities in the basement geometry (e.g. Mansy *et al*. 2003); or (4) irregular geometry of the backstop (Calassou *et al*. 1993; Kley 1999; Macedo & Marshak 1999).

All these geological features are present in the Subbetic units of the central Betics. Heterogeneities related to thickness variations of the sedimentary sequences are clearly demonstrated when the lithostratigraphic columns of Figure 3 are compared. Variations in thicknesses of the viscous substrate before the development of the fold-and-thrust belt, a first-order heterogeneity (Affolter & Gratier 2004; Likorish *et al*. 2004), are probably present throughout the Subbetic Domain. Indeed, according to Flinch *et al*. (1996), an initial diapiric emplacement of Triassic evaporitic rocks took place during the Mesozoic to Cenozoic passive margin evolution of the South Iberian Domain. Some of these diapirs rose to the surface at that time, as evaporite pebbles are observed in Subbetic rocks of Early Cretaceous age (Nieto *et al*. 2001). This no doubt resulted in the lateral thickness variation of the viscous substrate and even the disappearance of viscous material that was completely squeezed upwards. In such a setting, possibly reflecting the case of Sierra Gorda, lateral variations of the rheological properties of the substrate can produce oblique structures during progressive shortening (Bahroudi & Koyi 2003; Luján *et al*. 2003). Heterogeneities of both the basement geometry and the thickness of the Triassic evaporitic layer can be related to the normal faults that developed during the passive margin stage of the South Iberian Domain. Some of these faults have been drawn on the large-scale cross-section of Figure 2, although their exact position is unknown. During the tectonic inversion, some of these faults could have acted as lateral ramps, which probably produced thrusts and associated folds oblique to the general trend. Finally, the geometry of the backstop that pushes the Subbetic deformed wedge (in the central Betics, the Alboran Domain) can be either a recess or a salient. In our case study, the outer boundary of the Alboran Domain internal zones forms a recess of at least 30 km below the Granada basin (compare the position of the Alboran Domain east and west of Granada; Figs 1 and 2). This recess is precisely occupied by the north–south-trending oblique structure of Sierra Gorda. The substrate of the Sierra Gorda thrust system, which does not crop out, is probably brittle, or may have consisted of a very thin layer of viscous Triassic evaporitic rocks. Indeed, the well-determined vergence of the thrust system is characteristic of such a brittle substrate (Liu *et al*. 1992). Moreover, the strength of the folded sequence forming Sierra Gorda is much higher than that of most of the central Subbetic units. The highly competent early Jurassic unit at the base of Sierra Gorda brittle sequence reaches 1200 m in thickness, whereas around Alcalá or Priego, the same unit is only 275 m thick (Fig. 3). This very strong layer probably prevented the formation of superimposed folding in Sierra Gorda even if it were in a favourable situation. All these factors (presence of a recess, type of substrate and strength) are probably determinant for the origin of an anomalous trend in the Sierra Gorda thrust system within the central Betics. Finally, as will be discussed below, we are probably looking at the original orientation of Sierra Gorda thrust system, as only very little vertical-axis rotation was found from palaeomagnetic data (Villalaín *et al*. 1994).

Any of these factors (heterogeneities in the substrate, in the folded sequence, in the basement geometry or irregular backstop geometry), or a combination of them, would enhance the nucleation of oblique folds and thrusts within an NE–SW- to ENE–WSW-trending Subbetic wedge, in the earliest stages of the progressive deformation. These structures were not very frequent, as the map of the Subbetic structural trend shows no more then about 10 of them (Fig. 2). The deformed wedge detached from the Herynian basement during an initial NW–SE- to NNW–SSE-trending compression, in agreement with the present position of the Alboran Domain front, east of Granada (Figs 1 and 2). The initial structural trend of the Subbetic wedge, as the Alboran Domain front, was probably NE–SW trending in the central Betics, as late, slight clockwise rotations have been found by palaeomagnetic studies (see below). Some of these oblique structures can be generated at a high angle to the main fold trend. It may be noted that the anomalous north–south trend of Sierra Gorda is almost at right angles to the normal fold-and-thrust trend. Analogue modelling simulating the different geological situations discussed here showed that the angle between the main trend and the oblique structures generated in a deformed wedge can reach 90° (Calassou *et al*. 1993; Soto *et al*. 2002, 2003; Bahroudi & Koyi 2003; Luján *et al*. 2003; Likorish *et al*. 2004).

The second part of the proposed model deals with the folding of these early oblique structures, which requires near-parallelism between their trend and the later direction of shortening. The F_2 folds in the Alcalá and Priego area are NE–SW trending (Fig. 2). Consequently, the F_1 oblique folds had an NW–SE initial trend and were refolded during the same shortening episode that produced the main fold trend in the central Subbetic wedge, with a NE–SW compression direction. If the F_1 oblique folds were at a smaller angle to the main F_1 fold trend, a NNE–SSW to north–south compression should be invoked. In that case, all the previous folds that were not at right angles to the new compression direction should have rotated, either by hinge migration (Odonne & Vialon 1987) or by vertical-axis block rotation, which could have taken place along a detachment, favoured by the presence of viscous Triassic evaporites.

Some consequences for palaeomagnetic studies

The Mesozoic rocks of the Subbetic units have been the subject of several palaeomagnetic studies over the last 15 years (see review by Osete *et al*. 2004). In particular, Villalaín *et al*. (1994) established that the natural remanent magnetization of Upper Jurassic nodular limestones is dominated by a widespread and pervasive remagnetization of Neogene age. In fact, a heterogeneous pattern of rotations can be observed if the secondary, Neogene magnetization is incorrectly interpreted as a primary, Jurassic magnetization (Kirker & McClelland 1996; Villalaín *et al*. 1996). This gives rise to doubts regarding the reliability of previous palaeomagnetic studies in the Betics, which were mainly carried out in its western part (Platzman 1992; Platzmann & Lowrie 1992; Platt *et al*. 1994). With this background, Osete *et al*. (2004) carried out a palaeomagnetic investigation in the central and eastern Subbetics, to determine if Neogene remagnetization took place and to determine whether or not these remagnetized units were rotated. At the time of that study, however, neither the complexity of deformation in the Subbetic units nor the fold interferences were known. Therefore, it is useful to review the palaeomagnetic data in the light of the data presented in this paper.

In the area of Figure 2, Osete *et al*. (2004) showed that a widespread secondary remagnetization event took place, similar to that found in the western Betics by Villalaín *et al*. (1994). Four of these remagnetization vectors are taken from Osete *et al*. (2004) (ERJ, CY BR and ALJ), and the southernmost one from Villalaín *et al*. (1994) (Sierra Gorda, JGO). The relationships between the orientation of these vectors and the superimposition of structures allow for a better constraint of the timing of remagnetization, as the orientation of the remagnetization vector of samples ERJ, BR, ALJ and JGO is clearly independent of the structural trend (Table 1 and Fig. 2); whereas the remagnetization vector orientation is constant and NNE–SSW directed, the structural trend varies from north–south in Sierra Gorda to east–west NE of Lucena, passing through a NE–SW orientation for the BR and ALJ samples. There are two possible explanations: either the main deformation did not produce any rotation of a pre-tectonic remagnetization vector, a highly improbable hypothesis, or, more likely, the remagnetization imprinted a deformed wedge with a variable structural trend. Consequently, the remagnetization event would have occurred after the main deformation, that is, after the Aquitanian–Burdigalian boundary. Then, at the end of the deformation history, there was slight clockwise rotation of the whole area, of 10–15°.

To constrain the timing of remagnetization with respect to folding, a fold test was performed by Villalaín *et al*. (1994) and Osete *et al*. (2004) on three samples (ALJ, BRJ and JGO of Table 1). Unfortunately, in the light of the data presented in this paper (which indicate main folding followed by a tightening of the structures) these fold-test findings are ambiguous. According to Osete *et al*. (2004), remagnetization was acquired after 70% and 80% of folding in samples ALJ and BRJ, respectively. Both are situated along ENE–WSW folds, and two solutions are compatible with these data: (1) remagnetization during the main folding, and hence occurring at the Aquitanian–Burdigalian boundary; or (2) remagnetization after the main folding, and tightening of the folds, from Late Burdigalian time onwards. In fact, a few kilometres SW of the ALJ sampling site, near Iznájar (Fig. 2), Tortonian deposits seal F_1 main NE–SW-trending folds, and in turn, form an open syncline (with an interlimb angle of 140°) with the same trend (Cano Medina & Ruiz Reig 1990*b*). In the Sierra Gorda sample (JGO), Villalaín *et al*. (1994) claimed that remagnetization preceded the main folding. The fold test was performed using two sites situated in the same limb of the main, easternmost slice shown in cross-section C–C′ of Figure 3. It was found that their respective bedding planes show only slight difference in orientation (27/052 and 24/025; see Villalaín *et al*. 1994, table 1). This minor variation of bedding orientation attributed to the main contractional event could be due to other factors, such as tilting associated with late faults. Accordingly, the fold test is probably not reliable in this case.

Special attention should be paid to sample CY. This is the only sample from the study area to show a strong rotation of the remagnetization vector (*c*. 65° clockwise). This sample, together with samples ERJ1 and 2, is from the area of superimposed folding of Priego (Fig. 6). ERJ is from the southern limb of an east–west-directed F_1 anticline of 10 km length, whereas sample CY is from the eastern limb of an approximately north–south-directed F_1 anticline. These anticlines are not directly connected, as Triassic rocks appear between the two outcrops; yet, as noted above, the variation of the main structural trend is related to the presence of an F_2 fold, whose axial trace is shown in Figure 6. This fold produced a rotation of the F_1 axial plane similar to the vertical-axis rotation of the remagnetization vector. This is in agreement with a remagnetization event later than the F_1 main folding and before the F_2 folding. Unfortunately, in this area, no Miocene sediments are present to constrain the exact timing of fold superimposition, but this is a key area in which to obtain more samples for future palaeomagnetic studies.

The Subbetic Domain of the central Betics and the structural evolution of the external zones around the Gibraltar Arc

The Miocene structural evolution of the Subbetic units of the central Betics depicted in this paper can be framed within the tectonic history of the northern branch of the Gibraltar Arc. The present-day structural trend observed throughout the Subbetic and Flysch Trough Domains is shown in Figure 7a. In the same map, the orientation of the palaeomagnetic remagnetization vector in the western Betics is drawn according to Villalaín *et al*. (1994, 1996) and Kirker & McClelland (1996). It should be emphasized that Osete *et al*. (2004) suggested that remagnetization was synchronous throughout the Subbetic Domain, which represents an important milestone for any timing of the deformation.

Figure 7a shows that, in the western Betics, the remagnetization vectors were systematically rotated clockwise, about 70–80°; there, Crespo-Blanc & Campos (2001) showed that the main deformation episode, and probably the rotations, took place during the Late Burdigalian to Langhian age interval. Consequently, remagnetization would be pre-Langhian according to its relationship with the structure of the western Betics, and post-early Burdigalian on the basis of its relationship with the structure of the central Betics. All these structural and palaeomagnetic data, combined, lead to the sketches shown in Figure 7b–d, which represent three stages of the structural evolution of the northern branch of the Gibraltar Arc, from Early Burdigalian to Late Serravallian time.

By Early Burdigalian times (Fig. 7b), the structure of the Subbetic Domain fold-and-thrust wedge of the central Betics was nearly completed, as shown in this paper. In the western Betics, in contrast, sediments were still deposited on the South Iberian palaeomargin (Aquitanian to early Burdigalian flysch-type sediments on top of the most internal Subbetic sequence; Dubois & Magné 1972) and in the Flysch Trough Domain (supra-Numidian marls on top of the Numidian quarzites, early Burdigalian in age; Esteras *et al*. 1995). The erosion of the mountain front gave rise to the Late Burdigalian conglomerates observed in piggyback

Table 1. *Remagnetization vector v. structural trend in the Subbetic Domain of the central Betics*

Sample	Remagnetization vector (D/I)	Structural trend in the sampling area	Fold test
ERJ1	025/74	086	Not made
ERJ2	359/47		Not made
CYB	066/47	013	Not made
CYK	061/49		Not made
BRJ	004/58	082	Remagnetization after 80% of folding
ALJ	010/53	068	Remagnetization after 70% of folding
JGO	023/46	150	Pre-folding remagnetization

Remagnetization vector measured in the central Betics. Orientation given as declination/inclination (D/I). The structural trend has been estimated from the orientation of structures of several kilometres scale around the area of sampling. The palaeomagnetic data, together with the fold-test results, are taken from Villalaín *et al*. (1994, sample JGO) and Osete *et al*. (2004, the remaining samples).

basins such as that of Alcalá. The main trend of this deformed wedge was probably NE–SW, as the remagnetization vector recorded a 10° clockwise mean rotation. Oblique structures such as that of Sierra Gorda probably formed at that time. Meanwhile, in the internal part of the Gibraltar Arc, a low-angle normal fault system affected the Alboran Domain, with a tectonic transport direction towards the NNW in present coordinates (Contraviesa normal fault system; García-Dueñas *et al*. 1992; Crespo-Blanc *et al*. 1994). Accordingly, this Domain acted as a backstop that pushed the palaeomargin units.

Figure 7c illustrates the possible geological situation in Langhian time, immediately after the remagnetization(?), which, in the central Betics, imprinted all the structures regardless of their orientation. Meanwhile, in the western Betics, the Flysch Trough was totally obliterated. Together with the most internal zone of the Subbetic Domain, it was organized as a deformed wedge. If the remagnetization vector recorded the total vertical-axis rotation undergone by the structures, in the western Betics, the original structural trend should have been north–south to NNW–SSE directed, as late clockwise rotations of 70–80° have been inferred. This episode of shortening in the external zones *sensu lato* was synchronous with extension in the internal part of the Gibraltar Arc. Indeed, at that time, an extensional fault system with a west to SW tectonic transport direction affected the Alboran Domain (Filabres normal fault system; García-Dueñas *et al*. 1992). In Figure 7c, the central and western Betics are linked through the above-mentioned dextral strike-slip corridor, situated south of Sierra Gorda area, which developed between Late Burdigalian and Early Tortonian time.

Figure 7d illustrates how the structures have rotated clockwise at Late Serravallian time: very slightly in the central Betics, and to a greater extent in the western Betics. In the central Betics, this rotation could be contemporaneous with the compression that produced superimposed folding and the rotation of the remagnetization vector in the Priego area (Fig. 6). This differential rotation is accompanied by the formation of the major westernmost salient of the Gibraltar Arc, made up of the Subbetic and Flysch Trough Domains and the outer boundary of the Alboran Domain. In this salient, Balanyá *et al*. (2007) has shown that a partition of the deformation during arc formation took place, with the development of structures accommodating suborthogonal shortening (folds and thrusts) and structures accommodating arc-parallel stretching such as distributed minor structures, normal faults and conjugate strike-slip faults. Both types of faults have been drawn in the map of Figure 7.

The model proposed in this paper differs from that of Platt *et al*. (2003, fig. 13), in which the main deformation is contemporaneous throughout the Subbetic Domain and in which the convergence of the backstop represented by the Alboran Domain is constant and WNW directed throughout the deformation event. Obviously, the three sketches of Figure 7a–c are only approximations, in particular concerning the position of the Flysch Trough Domain. Although they require some refinement, they may encourage discussion of the tectonic history of a domain whose structural evolution is generally sketched as a compressional front sweeping the external Betics area during Miocene times. At lithospheric scale, the westward migrating arc with outward divergent folding and thrusting associated with a coeval extension in the inner part of the Gibraltar Arc proposed in this model, may fits any asymmetrical geodynamic model of the western Mediterranean, such as mantle delamination (e.g. García-Dueñas *et al*. 1992; Seber *et al*. 1996; Comas *et al*. 1999) or slab roll-back (e.g. Royden 1993; Michard *et al*. 2002; Faccenna *et al*. 2004).

Conclusions

(1) The Subbetic units of the central Betics consist of a deformed wedge of sedimentary rocks derived from the South Iberian palaeomargin. Shortening produced folding, thrusting and nappe-stacking during Miocene times. Their structural trend is mainly NE–SW to ENE–WSW, although anomalous areas with different trends can be observed.

(2) The deformation style of the thrust sheets is strongly controlled by the rheology of the lithostratigraphic sequences involved. The rheological profiles generally include a viscous layer of evaporitic rocks at the bottom, and a carbonate sequence whose competence varies with the location. In most areas, the structural style is characterized by folds and thrusts that show no preferred vergence, generally defining box-folds with associated pop-up and pop-down structures.

(3) Oblique structures are present in the Subbetic deformed wedge, and superimposed buckle folding is described for the first time in the study area. The origin of oblique structures could be related to heterogeneities of the substrate or the folded sequence, related to the Hercynian basement geometry or caused by an irregular backstop geometry; or to a variation of the compressional direction during progressive deformation. Concerning the origin of the superimposed buckle folding, it is suggested that some of the oblique folds and thrusts that developed locally in the earliest stages of the progressive deformation were subsequently folded, as a result of local variation of the stress field orientation, until there was near-parallelism of the fold trend and the maximum compression axis.

(4) The relationships of Miocene sediments deposited in piggyback basins show that the NE–SW- to ENE–WSW-trending main folds developed close to the Aquitanian–Burdigalian transition. It is suggested that although the so-called F_2 folds may have tightened the superimposed structures during Middle and Late Miocene times, the interference probably began during the main folding episode.

(5) A revision of the palaeomagnetic data published in previous papers, in light of the data presented here, in conjunction with a model of structural evolution of the Subbetic units of the western Betics, leads us to constrain the timing of the widespread, secondary remagnetization event that characterizes the Subbetic unit rocks within the Burdigalian–Langhian time interval. It also helps establish milestones in the tectonic evolution of the external zones of the northern branch of the Gibraltar Arc.

This study was supported by grant BTE2003-05057-C02 (Spain). D. Frizon de Lamotte, J. L. Simón and M. Durand-Delga are gratefully acknowledged for their comments. We also thank J. Sanders for reviewing the English version.

References

Affolter, T. & Gratier, J.P. 2004. Map view retrodeformation of an arcuate fold-and-thrust belt: the Jura case. *Journal of Geophysical Research*, **109**, B03404, doi:10.1029/2002JB002270.

Alvaro, M., Hernández, A., Del Olmo, P. & Ruiz-Reig, P. 1991. *Geological map. Sheet Torres, 948, scale 1:50*. Instituto Tecnológico Geominero de España, Madrid.

Bahroudi, A. & Koyi, H.A. 2003. Effect of spatial distribution of Hormuz salt on deformation style in the Zagros fold and thrust belt: an analogue modeling approach. *Journal of the Geological Society, London*, **160**, 719–733.

Balanyá, J.C. & García-Dueñas, V. 1988. El cabalgamiento cortical de Gibraltar y la tectónica de Béticas y Rif. *In:* Vera, J.A. (ed.) *Actas Segundo Congreso Geológico de España (Simposios)*. Sociedad Geológica de España, Granada, 35–44.

Balanyá, J.C., Crespo-Blanc, A., Díaz-Azpiroz, M., Expósito, I., Luján, M. 2007. Structural trend line pattern and strain partitioning around the Gibraltar Arc accretionary wedge: insights as to the mode of orogenic arc building. *Tectonics* doi: 10.1029/2005TC001932.

Barba, A., Martín, A. & Piles, E. 1979. *Geological map. Sheet Colmenar, 1039, scale 1:50 000*. Instituto Tecnológico Geominero de España, Madrid.

Berástegui, X., Banks, C.J., Puig, C., Taberner, C., Waltham, D. & Fernàndez, M. 1998. Lateral diapiric emplacement of Triassic evaporites at the southern margin of the Guadalquivir Basin, Spain. *In:* Mascle, A., Puigdefabregas, C. & Fernàndez, M. (eds) *Cenozoic Foreland Basins of Western Europe*. Geological Society, London, Special Publications, **134**, 49–68.

Blankenship, C. 1992. Structure and palaeogeography of the External Betic Cordillera, southern Spain. *Marine and Petroleum Geology*, **9**, 256–264.

Bourgois, J. 1978. La transversale de Ronda (Cordillères Bétiques, Espagne). Données géologiques pour un modèle d'évolution de l'Arc de Gibraltar. *Annales Scientifiques de l'Université de Besançon*, **30**, 1–445.

Butler, R.W.H., Coward, H.P., Harwood, G.M. & Knipe, R. 1987. Salt. Its control on thrust geometry, structural style and gravitational collapse along the Himalaya mountain front in the Salt Range of northern Pakistan. *In:* O'Brien, J.-J. & Lerche, I. (eds) *Dynamical Geology of Salt and Related Structures*. Academic Press, London, 399–418.

Calassou, S., Larroque, C. & Malavieille, J. 1993. Transfer zones of deformation in thrust wedges: an experimental study. *Tectonophysics*, **221**, 325–344.

Cano Medina, F. & Ruiz Reig, P. 1990a. *Geological map. Sheet Ardales, 1038, scale 1:50 000*. Instituto Tecnológico Geominero de España, Madrid.

Cano Medina, F. & Ruiz Reig, P. 1990b. *Geological map. Sheet Rute, 1007, scale 1:50 000*. Instituto Tecnológico Geominero de España, Madrid.

Comas, M.C. 1978. *Sobre la geología de los Montes orientales: sedimentación y evolución paleogeográfica desde el Jurásico hasta el Mioceno inferior (Zona Subbética, Andalucía)*. PhD thesis, Universidad del País Vasco, Bilbao.

Comas, M.C., García-Dueñas, V., Navarro, F. & Ruiz, P. 1986. *Geological map. Sheet Moreda, 992, scale 1:50 000*. Instituto Tecnológico Geominero de España, Madrid.

Comas, M.C., Platt, J.P., Soto, J.I. & Watts, A.B. 1999. The origin and tectonic history of the Alboran Basin: insights from Leg 161 results. *In:* Zahn, R., Comas, M.C. & Klaus, A. (eds) *Proceedings of the Ocean Drilling Program, Scientific Results, 161*. Ocean Drilling Program, College Station, TX, 555–580.

Costa, E. & Vendeville, B.C. 2002. Experimental insights on the geometry and kinematics of fold-and-thrust belts above weak, viscous evaporitc décollement. *Journal of Structural Geology*, **24**(2), 1729–1739.

Cotton, J. & Koyi, H. 2000. Modeling of thrust front above ductile and frictional detachments: application to structures in the Salt Range and Potwar Plateau, Pakistan. *Geological Society of America Bulletin*, **112**(3), 351–363.

Crespo-Blanc, A. & Campos, J. 2001. Structure and kinematics of the South Iberian paleomargin and its relationship with the Flysch Trough units: extensional reactivation within the Gibraltar Arc fold-and-thrust belt (western Betics). *Journal of Structural Geology*, **23**(10), 1615–1630.

Crespo-Blanc, A. & Frizon de Lamotte, D. 2006. Structural evolution of the external zones derived from the Flysch Trough and the South Iberian and Maghrebian paleomargins around the Gibraltar Arc: a comparative study. *Bulletin de la Société Géologique de France*, **177**(5), 267–282.

Crespo-Blanc, A., Orozco, M. & García-Dueñas, V. 1994. Extension versus compression during the Miocene tectonic evolution of the Betic Chain. Late folding of normal fault systems. *Tectonics*, **13**(1), 78–88.

Dercourt, J., Zonenshain, L.P., Ricou, L.E. *et al.* 1986. Geological evolution of the Tethys belt from the Atlantic to the Pamirs since the Lias. *Tectonophysics*, **123**, 241–315.

Díaz de Neira, J.A., Enrile Albir, A., Hernaiz Huerta, P.P. & López Olmedo, F. 1991a. *Geological map. Sheet alcalá La Real, 990, scale 1:50 000*. Instituto Tecnológico Geominero de España, Madrid.

Díaz de Neira, J.A., Enrile Albir, A., Hernaiz Huerta, P.P. & López Olmedo, F. 1991b. *Geological map. Sheet Valdepeñas de Jaén, 969, scale 1:50 000*. Instituto Tecnológico Geominero de España, Madrid.

Díaz de Neira, J.A., Enrile Albir, A., López Olmedo, F. & Hernaiz Huerta, P.P. 1991c. *Geological map. Sheet Huelma, 970, scale 1:50 000*. Instituto Tecnológico Geominero de España, Madrid.

Dubois, M. & Magné, J. 1972. Présence de Burdigalien dans la région d'Ubrique (Province de Cadix, Espagne méridionale). *Annales Scientifiques de l'Université de Besançon*, **3**(17), 113–116.

Durand-Delga, M., Rossi, P., Olivier, P. & Puglisi, D. 2000. Situation structurale et nature ophiolitique de roches basiques jurassiques associées aux flyschs maghrébins du Rif (Maroc) et de Sicile (Italie). *Comptes-Rendus de l'Académie des Sciences, Earth and Planetary Sciences*, **331**, 29–38.

Esteras, M., Feinberg, H. & Durand-Delga, M. 1995. Nouveaux éléments sur l'âge des grès numidiens de la nappe de l'Aljibe (Sud-Ouest de l'Andalousie, Espagne). *In:* Puego, J.M. (ed.) *Actas del IV Coloquio Internacional sobre el Enlace Fijo del Estrecho de Gibraltar, Sevilla, SECEG, Madrid*, **2**, 205–215.

Estévez, A., Rodríguez-Fernández, J., Sanz de Galdeano, C. & Vera, A. 1982. Evidencia de una fase compresiva de edad Tortoniense en el sector central de las Cordilleras Béticas. *Estudios Geológicos*, **38**, 55–60.

Faccenna, C., Piromallo, C., Crespo-Blanc, A., Jolivet, L. & Rosetti, F. 2004. Lateral slab deformation and the origin of the western Mediterranean arcs. *Tectonics*, **23**, TC1012, doi:10.1029/2002TC001488.

Fernàndez, M., Berástegui, X., Puig, C., García-Castellanos, D., Jurado, M.J., Torné, M. & Banks, C. 1998. Geophysical and geological constraints on the evolution of the Guadalquivir foreland basin, Spain. *In:* Mascle, A., Puigdefabregas, C. & Fernàndez, M. (eds) Geological Society, London, Special Publications, **134**, 29–48.

Flinch, J., Bally, A. & Wu, S. 1996. Emplacement of a passive-margin evaporitic allochthon in the Betic Cordillera of Spain. *Geology*, **14**(1), 67–70.

Frizon de Lamotte, D., Andrieux, J. & Guézou, J.C. 1991. Cinématique des chevauchements néogènes dans l'Arc bético-rifain: discussion sur les modèles géodynamiques. *Bulletin de la Société Géologique de France*, **162**, 611–626.

Frizon de Lamotte, D., Crespo-Blanc, A., Saint-Bézar, B., *et al.* 2004. TRANSMED—transect I (Betics, Alboran Sea, Rif, Moroccan Meseta, High Atlas, Jbel Saghro, Tindouf basin): a description of the section and data sources. *In*: Cavazza, W., Roure, F.M., Spakman, W., Stampfli, G.M. & Ziegler, P.A (eds) *The TRANSMED Atlas: the Mediterranean Region from Crust to Mantle*. CD-ROM. Springer, Berlin.

García-Cortés, A. 1991. *Geological map. Sheet Alcaudete 968, scale 1:50 000*. Instituto Tecnológico Geominero de España, Madrid.

García-Dueñas, V., Balanyá, J.C. & Martínez-Martínez, J.M. 1992. Miocene extensional detachments in the outcropping basement of the northern Alboran Basin and their tectonic implications. *Geo-Marine Letters*, **12**, 88–95.

García-Hernández, M., López-Garrido, A.C., Rivas, P., Sanz de Galdeano, C. & Vera, J.A. 1980. Mesozoic palaeogeographic evolution of the external zones of the Betic Cordillera. *Geologie en Mijnbouw*, **59**, 155–168.

García-Hernández, M., López-Garrido, A.C. & Vera, J.A. 2004. El Prebético del sector central y afloramientos más occidentales. *In:* Vera, J.A. (ed.) *Geología de España*. Sociedad Geológica de España–Instituto Geológico y Minero de España, Madrid, 363–365.

Ghosh, S.K. & Ramberg, H. 1968. Buckling experiments on intersecting fold patterns. *Tectonophysics*, **5**, 89–105.

Ghosh, S.K., Mandal, N., Khan, D. & Deb, S.K. 1992. Modes of superposed buckling in single layers controlled by initial tightness of early folds. *Journal of Structural Geology*, **14**, 381–394.

Grujic, D. 1993. The influence of initial fold geometry on Type 1 and Type 2 interference patterns: an experimental approach. *Journal of Structural Geology*, **15**, 293–307.

Grujic, D., Walter, T. & Gärtner, H. 2002. Shape and structure of (analogue models) of refolded layers. *Journal of Structural Geology*, **24**, 1313–1326.

Guerrera, F., Martin-Algarra, A. & Perrone, V. 1993. Late Oligocene–Miocene syn-/late-orogenic successions in western and central Mediterranean chains from the Betic cordilleras to the southern Apennines. *Terra Nova*, **5**, 525–544.

Guezou, J.C., Frizon de Lamotte, D., Coulon, M. & Morel, J.L. 1991. Structure and kinematics of the Prebetic nappe complex (Southern Spain): definition of a 'Betic Floor Thrust' and implications in the Betic–Rif orocline. *Annales Tectonicae*, **1**, 32–48.

Hernaiz Huerta, P.P., Díaz de Neira, J.A., Enrile Albir, A. & López Olmedo, F. 1991. *Geological map. Sheet Lucena 989, scale 1:50 000*. Instituto Tecnológico Geominero de España, Madrid.

IGME 1987. *Contribución de la exploración petrolífera al conocimiento de la Geología de España*. Instituto Geológico y Minero de España, Madrid.

Junta de Andalucía 1985. *Mapa Geologico-Minero de Andalucía, scale 1:400 000*. Consejería de Economía e Industria, Sevilla.

Kirker, A. & McClelland, E. 1996. Application of net tectonic rotations and inclination analysis to a high-resolution paleomagnetic study in the Betic Cordillera. *In:* Morris, A. & Tarling, D.H. (eds) *Paleomagnetism and Tectonics of the Mediterranean Region*. Geological Society, London, Special Publications, **105**, 19–32.

Kirker, A. & Platt, J.P. 1998. Unidirectional slip vectors in the western Betic Cordillera: implications for the formation of the Gibraltar Arc. *Journal of the Geological Society, London*, **155**, 193–207.

Kley, J. 1999. Geologic and geometric constraints on a kinematic model of the Bolivian orocline. *Journal of South American Earth Sciences*, **12**, 221–235.

Likorish, W.H., Ford, M., Bürgisser, J. & Cobbold, P.R. 2002. Arcuate thrust systems in sandbox experiments: a comparison to the external arcs of the Western Alps. *Geological Society of America Bulletin*, **114**, 1089–1107.

Liu, H., McClay, K.R. & Powell, D. 1992. Physical models of thrust wedges. *In:*

McClay, K.R. (ed.) *Thrust Tectonics*. Chapman and Hall, London, 71–81.

López Olmedo, F., Díaz de Neira, J.A., Enrile Albir, A. & Hernaiz Huerta, P.P. 1991. *Geological map. Sheet Iznalloz, 991, scale 1:50 000*. Instituto Tecnológico Geominero de España, Madrid.

Luján, M., Storti, F., Balanyá, J.C., Crespo-Blanc, A. & Rossetti, F. 2003. Role of décollement material with different rheological properties in the structure of the Aljibe thrust imbricate (Flysch Trough, Gibraltar Arc): an analogue modelling approach. *Journal of Structural Geology*, **25**, 867–881.

Luján, M., Crespo-Blanc, A. & Balanyá, J.C. 2007. Flysch Trough thrust imbricate (Betic Cordillera): a key element of the Gibraltar Arc orogenic wedge. *Tectonics*, **25**, TC6001 doi: 10.1029/2005TC001910.

Lupiani, E., Soriano, J.M., Baena, J. & Pérez, A. 1988. *Geological map. Sheet Loja, 1025, scale 1:50 000*. Instituto Tecnológico Geominero de España, Madrid.

Macedo, J. & Marshak, S. 1999. Control on the geometry of fold–thrust belt salients. *Geological Society of America Bulletin*, **111**(12), 1808–1822.

Mansy, J.L., Manby, G.M. & Averbuch, O. *et al.* 2003. Dynamics and inversion of the Mesozoic Basin of the Weald–Boulonnais area: role of basement reactivation. *Tectonophysics*, **373**, 161–179.

Martín-Algarra, A. 1987. *Evolución geológica alpina del contacto entre las zonas internas y externas de la Cordillera Bética*. PhD thesis, University of Granada.

Martín-Algarra, A., Sanz de Galdeano, C. & Estévez, A. 1988. L'évolution sédimentaire miocène de la région au Nord de la Sierra Arana (Cordillères Bétiques) et sa relation avec la mise en place du bloc d'Alboran. *Bulletin de la Société Géologique de France*, **4**(1), 119–127.

Martínez del Olmo, W., García-Mallo, J., Serrano, A. & Suárez, J. 1984. Modelo tectonosedimentario del Bajo Guadalquivir. *In:* Pérez, P. (ed.) *Actas del I Congreso Geológico de España, Segovia*. 199–213.

Michard, A., Chalouan, A., Feinberg, H., Goffé, B. & Montigny, R. 2002. How does Alpine belt end between Spain and Morocco? *Bulletin de la Société Géologique de France*, **173**, 3–15.

Molina, J.M. & Ruiz-Ortiz, P. 1993. Discussion to 'Structure and palaeogeography of the External Betic Cordillera, southern Spain', by C. L. Blankenship. *Marine and Petroleum Geology*, **10**, 516–518.

Nieto, L.M., De Gea, G.A., Aguado, R., Molina, J.M. & Ruiz-Ortiz, P.A. 2001. Procesos sedimentarios y tectónicos en el tránsito Jurásico/Cretácico: precisiones bioestratigráficas (Unidad del Ventisquero, Zona Subbética). *Revista de la Sociedad Geológica de España*, **14**(1-2), 35–46.

Odonne, F. & Vialon, P. 1987. Hinge migration as a mechanism of superimposed folding. *Journal of Structural Geology*, **9**(7), 835–844.

Osete, M.L., Villalaín, J.J., Palencia, A., Osete, C., Sandoval, J. & García-Dueñas, V. 2004. New palaeomagnetic data from the Betic Cordillera: constraints on the timing and the geographical distribution of tectonic rotations in Southern Spain. *Pure and Applied Geophysics*, **161**, 701–722.

Platt, J. & Vissers, R.L.M. 1989. Extensional collapse of thickened continental lithosphere: a working hypothesis for the Alboran Sea and Gibraltar Arc. *Geology*, **17**, 540–543.

Platt, J., Allerton, S., Kirker, A. & Platzman, E. 1994. Origin of the western Subbetic Arc (South Spain): paleomagnetic and structural evidence. *Journal of Structural Geology*, **17**, 765–775.

Platt, J.P., Allerton, S., Kirker, A., Mandeville, C., Mayfield, A., Platzman, E.S. & Rimi, A. 2003. The ultimate arc: differential displacement, oroclinal bending and vertical axis rotation in the External Betic–Rif arc. *Tectonics*, **22**(3), 1017, doi:10.1029/2001TC001321.

Platzman, E.S. 1992. Paleomagnetic rotations and the kinematics of the Gibraltar Arc. *Geology*, **20**, 311–314.

Platzmann, E.S. & Lowrie, W. 1992. Palaeomagnetic evidences for rotation of the Iberian Peninsula and the external Betic Cordillera, southern Spain. *Earth and Planetary Science Letters*, **108**, 45–60.

Ramsay, J.G. 1967. *Folding and Fracturing of Rocks*. McGraw–Hill, New York.

Reicherter, K. 1993. To balance or not? Comment on 'Structure and palaeogeography of the External Betic Cordillera, southern Spain', by C. L. Blankenship. *Marine and Petroleum Geology*, **10**, 514–515.

Rodríguez-Fernández, J. 1982. *El Mioceno del sector central de las Cordilleras Béticas*. PhD thesis, University of Granada.

Royden, L.H. 1993. Evolution of retreating subduction boundaries formed during continental collision. *Tectonics*, **12**, 629–638.

Sanz de Galdeano, C., Martín Algarra, A., Vera, A. & Rivas, P. 1993. Comments on 'Structure and palaeogeography of the External Betic Cordillera, southern Spain', by C. L. Blankenship. *Marine and Petroleum Geology*, **10**, 518–521.

Seber, D., Barazangi, M., Ibenbrahim, A. & Demnati, A. 1996. Geophysical evidence for lithospheric delamination beneath the Alboran Sea and Rif–Betic mountains. *Nature*, **379**, 785–790.

Sengupta, S., Ghosha, S.K., Deba, S.K. & Khana, D. 2005. Opening and closing of folds in superposed deformations. *Journal of Structural Geology*, **27**, 1282–1299.

Sierro, F.J., González-Delgado, J.A., Dabrio, C.J., Flores, J.A. & Civis, J. 1996. Late Neogene depositional sequence in the foreland basin of Guadalquivir (SW Spain). *In:* Friend, P.F. & Dabrio, C.J. (eds) *Tertiary Basins of Spain. The Stratigraphic Record of Crustal Kinematics*. Cambridge University Press, Cambridge, 329–334.

Simón, J.L. 2004. Superposed buckle folding in the eastern Iberian Chain, Spain. *Journal of Structural Geology*, **26**, 1447–1464.

Skjernaa, L. 1975. Experiments on superimposed buckle folding. *Tectonophysics*, **27**, 255–270.

Sommaruga, A. 1999. Décollement tectonics in the Jura foreland fold-and-thrust belt. *Marine and Petroleum Geology*, **16**, 111–134.

Soria, J.M. 1994. Sedimentación y tectónica durante el Mioceno en la región de Sierra Arana–Mencal y su relación con la evolución geodinámica de la Cordillera Bética. *Boletín de la Sociedad Geológica de España*, **7**(3-4), 199–213.

Soria, J.M. 1998. La cuenca de antepaís Norbética en la Cordillera bética central (sector de Mencal): evolución tectosedimentaria e historia de la subsidencia. *Boletín de la Sociedad Geológica de España*, **11**(1-2), 23–31.

Soto, R., Casas, A.M., Storti, F. & Faccenna, C. 2002. Role of lateral thickness variations on the development of oblique structures at the Western end of the South Pyrenean Central Unit. *Tectonophysics*, **350**, 215–235.

Soto, R., Storti, F., Casas, A.M. & Faccenna, C. 2003. Influence of along-strike pre-orogenic sedimentary tapering on the internal architecture of experimental thrust wedges. *Geological Magazine*, **140**(3), 253–264.

Thiessen, R.L. & Means, W.D. 1980. Classification of fold interference patterns: a reexamination. *Journal of structural Geology*, **2**(3), 311–316.

Vera, J.A. 2000. El Terciario de la Cordillera Bética: estado actual de conocimientos. *Boletín de la Sociedad Geológica de España*, **13**(2), 345–373.

Vera, J.A. 2004. Zonas externas Béticas. *In:* Vera, J.A. (ed.) *Geología de España*. Sociedad Geológica de España–Instituto Geológico y Minero de España, Madrid, 354–389.

Villalaín, J.J., Osete, M.L., Vegas, R., García-Dueñas, V. & Heller, F. 1994. Widespread Neogene remagnetization in Jurassic limestones of the South-Iberian palaeomargin (Western Betics, Gibraltar Arc). *Physics of the Earth and Planetary Interiors*, **85**, 15–33.

Villalaín, J.J., Osete, M.L., Vegas, R., García-Dueñas, V. & Heller, F. 1996. The Neogene remagnetization in the western Betics: a brief comment on the reliability of paleomagnetic directions. *In:* Morris, A. & Tarling, D.H. (eds) *Paleomagnetism and Tectonics of the Mediterranean Region*. Geological Society of America, Special Papers, **105**, 33–41.

Watkinson, A.J. 1981. Patterns of fold interference: influence of early fold shapes. *Journal of Structural Geology*, **3**, 19–23.

Received 1 March 2006; revised typescript accepted 8 June 2006.
Scientific editing by Ian Alsop